



**HAL**  
open science

## A DFT study on the initial stage of thermal degradation of Poly(methyl methacrylate)/carbon nanotube system

Benoit Minisini, Emerson Vathonne, Carine Chivas-Joly, J. Lopez-Cuesta

### ► To cite this version:

Benoit Minisini, Emerson Vathonne, Carine Chivas-Joly, J. Lopez-Cuesta. A DFT study on the initial stage of thermal degradation of Poly(methyl methacrylate)/carbon nanotube system. *Journal of Molecular Modeling*, 2013, 19 (2), pp.623-629. 10.1007/s00894-012-1584-z . hal-04163121

**HAL Id: hal-04163121**

**<https://imt-mines-ales.hal.science/hal-04163121>**

Submitted on 27 Jul 2023

**HAL** is a multi-disciplinary open access archive for the deposit and dissemination of scientific research documents, whether they are published or not. The documents may come from teaching and research institutions in France or abroad, or from public or private research centers.

L'archive ouverte pluridisciplinaire **HAL**, est destinée au dépôt et à la diffusion de documents scientifiques de niveau recherche, publiés ou non, émanant des établissements d'enseignement et de recherche français ou étrangers, des laboratoires publics ou privés.

# A DFT study on the initial stage of thermal degradation of Poly(methyl methacrylate)/carbon nanotube system

Benoit Minisini · Emerson Vathonne · Carine Chivas-Joly · José-Marie Lopez-Cuesta

**Abstract** DFT calculations, with VWN exchange correlation functional and double numeric basis set, were used to evaluate the energies required for the scission reactions taking place in the initial stage of the thermal degradation of Poly(methyl methacrylate) (PMMA) in the presence of a carbon nanotube (CNT). Side group and main chain scissions were investigated. The results averaged from five configurations of pure PMMA (DP=5) were used as references and compared to the results obtained for the five same configurations of PMMA grafted on three carbon nanotubes of similar diameter (1.49 nm). The bond dissociation energies (BDE) of main chain scission evaluated for grafted PMMA was 4 % less endothermic than for pure PMMA. These results seemed independent of the tested chirality (11,11); (12,10) and (16,5) of the carbon nanotubes. Comparisons with the BDE of the weakest bonds due to intrinsic defaults (head to head and unsaturated end chain) were performed.

**Keywords** Bond dissociation energy · Carbon nanotubes · DFT · PMMA · Thermal degradation

B. Minisini (✉) · E. Vathonne  
ISMANS,  
44 Avenue F A Bartholdi,  
72000 Le Mans, France  
e-mail: bminisini@ismans.fr

C. Chivas-Joly  
LNE,  
29 Avenue Roger Hennequin,  
78197 Trappes Cedex, France

J.-M. Lopez-Cuesta  
CMGD—Ecole des Mines d'Alès,  
6 Avenue de Clavières,  
30319 Ales Cedex, France

## Introduction

Progress during the past 40 years by chemists, polymer and plastic manufacturers have made plastic materials ubiquitous in all sectors. Nevertheless, the formulations of commodity polymers still have to be improved upon particularly in the field of reaction or resistance to fire in spite of real progresses [1–3]. The halogenated flame retardants have been found to be good candidates to fulfill the delicate requirement cost/efficiency. However, these additives degrade the intrinsic properties of the polymers, and most of all represent a source of persistent organic pollutants [4]. Alternative solutions exist, as various phosphorous [5] and silicon [6] based molecules as well as mineral hydroxides or hydroxycarbonates [7]. These compounds may be used alone or in the presence of synergistic compounds [3, 8].

Coupled with the advent of nanotechnologies, abundant studies prepared over the past 20 years have shown that nanoparticles including carbon nanotubes (CNT) could improve the flammability of polymer nanocomposites [2, 9–12]. The couple polymethylmethacrylate (PMMA)/carbon nanotubes (CNT) has been the subject of intense studies aimed at understanding the mechanisms of thermal degradation and the reaction to fire in the presence of multi-walled (MWNT) [13–17] or single-walled (SWNT) [18–20]. This can be explained by the fact that the degradation mechanisms of pure PMMA are among the best documented [21] and can thus serve as a reference. Various explanations have been put forward on the role of CNTs. Some involve minor external factors such as the presence of iron nanoparticles [22], catalytic residues which can be present up to 25 % by mass in industrial carbon nanotubes. However, the interactions that occur between the polymer matrix and the nanoparticles seem to be the most influential. Kashiwagi et al. [18] were able to demonstrate the links between dispersion, increased viscosity of the melt and the

reduction of bubble formation during combustion and thus improving the protective role of the charred layer in a PMMA/SWNT system [18]. In this case, the carbon nanotubes would influence the dynamic behavior of the polymer chains thereby reducing the diffusion coefficient of radical species created during thermal degradation. Moreover, carbon nanotubes can also change the chemical reactions occurring in the condensed phase. Indeed, the chemical reactivity of carbon nanotubes has been considered in different studies dealing with the in situ polymerization of PMMA [23, 24]. The opening of  $\pi$  bonds existing on the surface of the nanotubes is generally involved in the chemistry of the carbon nanotubes [25]. However, chemically reactive sites, such as carbonyl, carboxyl or hydroxyl groups, are also present on the edge of open nanotubes, mainly after acid treatments which were used to purify the nanotubes from catalytic residues [26]. The presence of such oxygenated groups may play a role during the thermal degradation of PMMA which could be modified by the nanoparticle surface chemistry. As an example, the presence of methanol during the thermal degradation of a PMMA/titanium oxide nanoparticles system was explained by Laachachi et al. [27] through a chemical process involving the grafting of PMMA on the surface of nanoparticles using this type of group. Thus, specific chemical bonds would be susceptible to affect the mechanisms of thermal degradation for a PMMA/CNT system. Among the descriptor of thermal degradation accessible via quantum calculations, the bond dissociation energies are important since they can be linked to the temperature of half decomposition [28], the energy of activation [28, 29] and to the enthalpy of combustion and gasification [30, 31].

Consequently, the aim of this work is to contribute to the understanding of the degradation mechanisms of the PMMA/CNT system using molecular modeling tools based on the density functional theory (DFT). The various energy components for computable models of pure PMMA were quantitatively evaluated, and compared to those obtained for models of PMMA chains grafted on different carbon nanotubes.

## Methods

The aim of this study is to compare the different homolytic dissociation energies taking place during the thermal degradation of pure and grafted PMMA. An oligomer chain, with a degree of polymerization (DP) of 5, of an isotactic PMMA was built with Materials Studio 4.4 interface [32], the repeat unit is given in Fig. 1. With such a DP, a configurational study can be performed, while maintaining a reasonable calculation time. From this chain, five conformations were randomly extracted from a trajectory of 500 ps ( $10^{-12}$ s), after

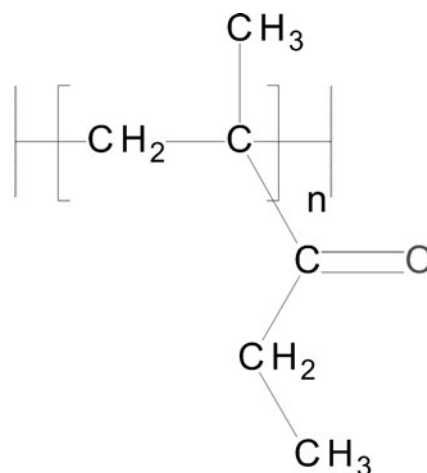
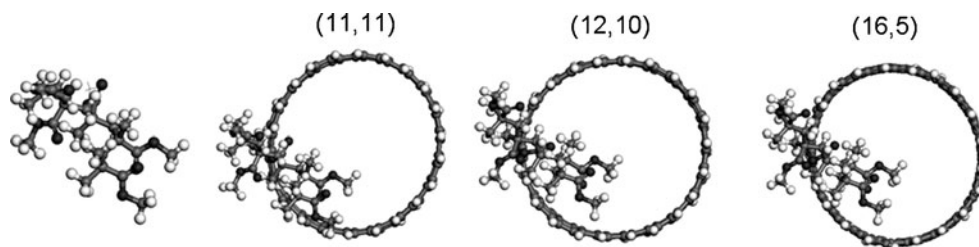


Fig. 1 Repeat unit of Poly(methyl methacrylate) (PMMA)

an equilibration of 200 ps, obtained by classical molecular dynamics performed in a NVT ensemble (number of atoms, volume and temperature are kept constant) at 600 K using the force field COMPASS [33] in Discover<sup>®</sup> code. The atomic positions of these five PMMA models were then optimized using classical molecular mechanics followed by quantum mechanics through the DMOL3<sup>®</sup> [34, 35] code available via Materials Studio v4.4<sup>®</sup> interface developed by Accelrys Inc. These chains were then grafted with the methoxycarbonyl group of the third monomer unit on the edge of a carbon nanotube. Multiwall CNT are extensively used in experimental or industrial nanocomposites. However, due to the number of atoms required to model such systems, the simulation times can easily become unreasonable when treated at ab initio level. Consequently, a singlewall CNT (SWNT) was chosen for this study. From a practical point of view, the SWNT are generally characterized by their average diameters, 1.5 nm is a common value given by commercial suppliers. However, the standard deviation is rarely given and can be large as shown by Cipriano et al. [13]. From an atomistic point, it is possible to evaluate a theoretical diameter from the chiral indices ( $n,m$ ) and the lattice constant  $a$  of graphite [36]. In this study, three different SWNTs with a chirality of (12,10), (11,11) and (16,5) were modeled to assess the influence of these parameters at constant theoretical diameter (1.49 nm). This diameter was chosen because it represented an average diameter of the SWNT when given by the majority of the 30 industrial suppliers of SWNT we reviewed. It is important to remember [13] that a simple average diameter is insufficient to accurately describe the distribution of diameter of industrial carbon nanotubes. We used a finite model which was required to saturate the dangling bonds with hydrogen atoms. The different bonds of interest in this study are shown in Fig. 2.

Bond 1 was involved in the homolytic scission of the methoxycarbonyl lateral group whereas bond 2 and bond 3 represented the bonds between carbon atoms within the

**Fig. 2** Optimized geometries at LDA/DN level of theory for one configuration of pure and grafted PMMA on the different studied carbon nanotubes (*white* = hydrogen atom, *light gray* = carbon atom, *dark gray* = oxygen atom)



chain. The difference between the two bonds was only their position relative to the grafting point. The energy of these different bonds was compared to that of known defects in synthesized PMMA. The synthesis can generate head-head chain defects in the PMMA chains. To evaluate the binding energy of such defects, we created five models with a head-head chain defect. The different energies were evaluated using the density functional theory (DFT) [37, 38]. The equations were solved using the spin unrestricted formalism and the VWN [39] functional to take into account the exchange correlation potential in the local density approximation (LDA). The wave-function was modeled using a double numeric (DN) basis set. Truncation in the real space of  $3 \text{ \AA}$  was set for the numerical integration while the SCF cycle was considered to have converged when the difference between the two successive iterations gave a quadratic average of the surface charge density below  $10^{-4}$  Hartree. The convergence criteria on energy, gradient and displacement were set at  $10^{-4}$ ,  $2.10^{-2}$  and  $5.10^{-2}$  ua respectively. All the energies, were evaluated at 0 K, ignoring the zero point energy and thermal correction.

## Results and discussion

Energy is the property accessible via quantum calculations requiring the least amount of approximations. Nonetheless, the accuracy depends on numerous parameters such as the exchange correlation treatment, basis set, convergence threshold, algorithms, and as bond dissociation energies can be used directly or indirectly as input parameters in mesoscopic model, the error should be as small as possible. Consequently, there has been considerable worldwide research to develop and assess new ab initio procedures. In spite of the formidable effort made by the scientists in this field, obtaining accurate results for polymers remains challenging. The reason is that accurate methods can be applied only on small molecules with a geometry coming from the

optimization of the atomic positions in a vacuum or solvent. This strategy was used by Stoliarov et al. [40] to evaluate the reactions from the decomposition of PMMA. They optimized the 2-hydroxy-2-methyl-pentan-2-one molecule to represent a fragment of PMMA and used the CBS-QB3 method known for its accuracy in the evaluation of energy. Conforti and Garrison [41] used the same method to calculate the energies of the reactions taking place during the UV degradation of PMMA. However, the spatial configuration of polymer fragments in the vacuum due to steric hindrances and long range interactions is completely different from that in the polymer bulk. Hence, in this work we have adopted another strategy in which we have averaged our properties on five conformations of atomic composition  $C_{25}H_{42}O_{10}$ . In our case, the energy of the most stable conformation is  $64 \text{ kJ mol}^{-1}$  less than the most energetic conformation. The energy of combustion for the different conformation was determined to assess the effect of the conformations on the results. An average value of  $-19.18 \text{ kJ/g}$  of PMMA or  $-9.86 \text{ kJ/g}$  of  $O_2$  was obtained with an error deviation of  $0.04 \text{ kJ/g}$  of PMMA and  $0.02 \text{ kJ/g}$  of  $O_2$  respectively. Our result was less exothermic than the experimental values measured in a oxygen bomb calorimeter according to the standard procedure ASTM D2382-88, by Walters et al. [30]:  $-26.75 \pm 0.14$  and  $-26.86 \pm 0.61 \text{ kJ/g}$  for PMMA supplied by Aldrich Chemical Company, Inc. and Polycast acrylic respectively. The discrepancy between the calculated and the experimental results can be partially understood by the fact that LDA overestimates the binding energy. The most important point is the fact that the experimental uncertainty, superior to  $0.1 \text{ kJ/g}$  of  $O_2$ , is higher than the standard deviation obtained from our five configurations. In addition, from our calculations, Table 1 indicates the bond dissociation energies (BDE) of the different bonds described in the Fig. 2.

The values given in the table are the averages obtained on the BDE of the five configurations. The BDE evaluated from the configurations of the lowest energies coming from the optimizations of the different product and reactant models

**Table 1**  $\Delta H_d(0 \text{ K})$  ( $\text{kJ mol}^{-1}$ ) for different bonds described in Fig. 2 for pure and grafted PMMA, average on five configurations, in brackets are given the values for the lowest energy configurations for products and reactants

	Pure	(11,11)	(12,10)	(16,5)
Bond 1	461±11 (476)	446±3 (444)	398±27 (393)	401±5 (398)
Bond 2	411±21 (423)	394±8 (381)	384±20 (384)	385±10 (371)
Bond 3	411±21 (423)	402±27 (399)	415±21 (419)	414±4 (403)

are given in brackets. The error reached as much as 5 % of the BDE which made it difficult to draw absolute conclusions with such a small sample size. Anyway, a trend can be highlighted which seems in agreement with the results coming from the configurations of the lowest energies. First of all, we saw that for pure PMMA, the BDE of bond 1 was, on average,  $50 \text{ kJmol}^{-1}$  more endothermic than bond 2, whereas from the configurations of lowest energies, the discrepancy was  $53 \text{ kJmol}^{-1}$ . This value was close to  $48 \text{ kJmol}^{-1}$ , found by Stoliarov et al. [40] for the BDE evaluated from a monomer unit of PMMA using the CBS-QB3 method. Consequently, it can be considered that our results are rather satisfactory even if the LDA, taking into account all the approximations, led to absolute values higher than the common bond dissociation energies of C-C ranging from  $350$  to  $380 \text{ kJmol}^{-1}$  [42].

Once the polymer chains were grafted on the carbon nanotube, their conformations evolved due to two effects. On one hand, a new bond was created after grafting and consequently this new electronic distribution led to new forces. On the other hand, steric hindrance led to new distortions. Figure 3 presents one out of the five configurations model of pure and grafted PMMA on the three carbon nanotubes.

This figure shows that the global geometry of the conformers was not completely affected by the grafting. However, to quantify the impact of grafting on the geometry of the conformers, we determined the radius of gyration ( $R_g$ ) defined as the square root of the mass average of  $r_i^2$  for all the mass elements of mass  $m_i$ , where  $r_i$  is the distance of the element from the center of mass. Only the atoms in common with the four structures were taken into account for the calculation. For the five models of pure PMMA, an average of  $40 \pm 01 \text{ \AA}$  was obtained. For three models, an increase of  $R_g$ , less than 5 % regardless of the chirality was observed. The carbon nanotubes were also affected by the grafting. To quantify this effect, the distributions of the C-C bond

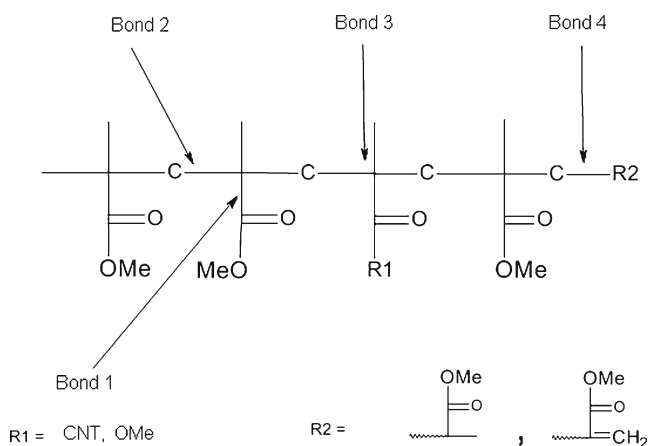


**Fig. 3** Model of PMMA (DP 5) with the different studied bonds

distances obtained for the optimized models were established (Fig. 4).

The mean C-C distance in the pure carbon nanotube was of  $1.41 \pm 01 \text{ \AA}$ , compared to the theoretical value of  $1.42 \text{ \AA}$ , and was independent of the chirality. Some peaks around  $1.37 \text{ \AA}$  were visible on all of the graphs. The carbon atoms involved in these bonds were those present at the end of carbon nanotubes and saturated by hydrogen atoms. We can conclude that the distributions are a function of the chirality. Indeed, for the (11,11) carbon nanotube, the discretization is more pronounced than that of the two others. The global shapes of the distributions were not drastically affected by the grafting or by the bond dissociation even if some discrepancies were visible. Moreover, the variations of the electrostatic potential on the hydrogen atoms at the opposite end of the grafting point were less than 1 % before and after the scissions. Consequently, we can assume that the number of atoms used to define our finite size models of carbon nanotube is sufficient and will not qualitatively affect our results.

Among the different bonds, bond 2 seemed the most affected by the presence of the nanotubes. The BDE (bond 2) was on average lower by 4 % less than for pure PMMA. It can be emphasized that it corresponds to a short range effect since the BDE (bond 3) is statistically equivalent to the BDE for pure PMMA. Consequently, the grafting of PMMA on carbon nanotubes creates weak C-C bonds comparatively to those of pure PMMA without defaults. Concerning the effect of the chirality, it is difficult to draw any conclusion from our results as the standard deviation is too significant. However, if such effects existed, the differences would be around  $10 \text{ kJmol}^{-1}$  and would be difficult to observe experimentally.

The influence of the different chiralities was more visible on the BDE (bond 1). A difference of behavior can be observed between (12,10) and (16,5) on one hand and (11,11) on the other. For the last one, the decrease in energy was around  $20 \text{ kJmol}^{-1}$  in comparison to  $60 \text{ kJmol}^{-1}$  for the two other nanotubes. This difference in energy can be explained by the fact that after bond scission the optimization of the atomic positions does not converge toward the same chemical structures. Indeed, after scission of the methoxycarbonyl group, one of the reactant should be the  $\text{CNT-O-(C=O)}^\bullet$  radical. However, after an optimization of the atomic positions, the bond lengths CNT-O- and -O-(C=O) $^\bullet$  were both close to  $1.42 \text{ \AA}$  for (11,11) whereas, for (12,10) and (16,5), we measured CNT-O- to be  $1.28 \text{ \AA}$  and -O-(C=O) $^\bullet$  to be superior to  $2 \text{ \AA}$ . Consequently, for (12,10) and (16,5) we had a  $\text{CNT-O}^\bullet \text{ C=O}$  radical which meant that a molecule of carbon monoxide was released in addition to the polymer bond scission.

It is commonly accepted that the thermal degradation of pure PMMA is initiated by scission of the weakest bonds.

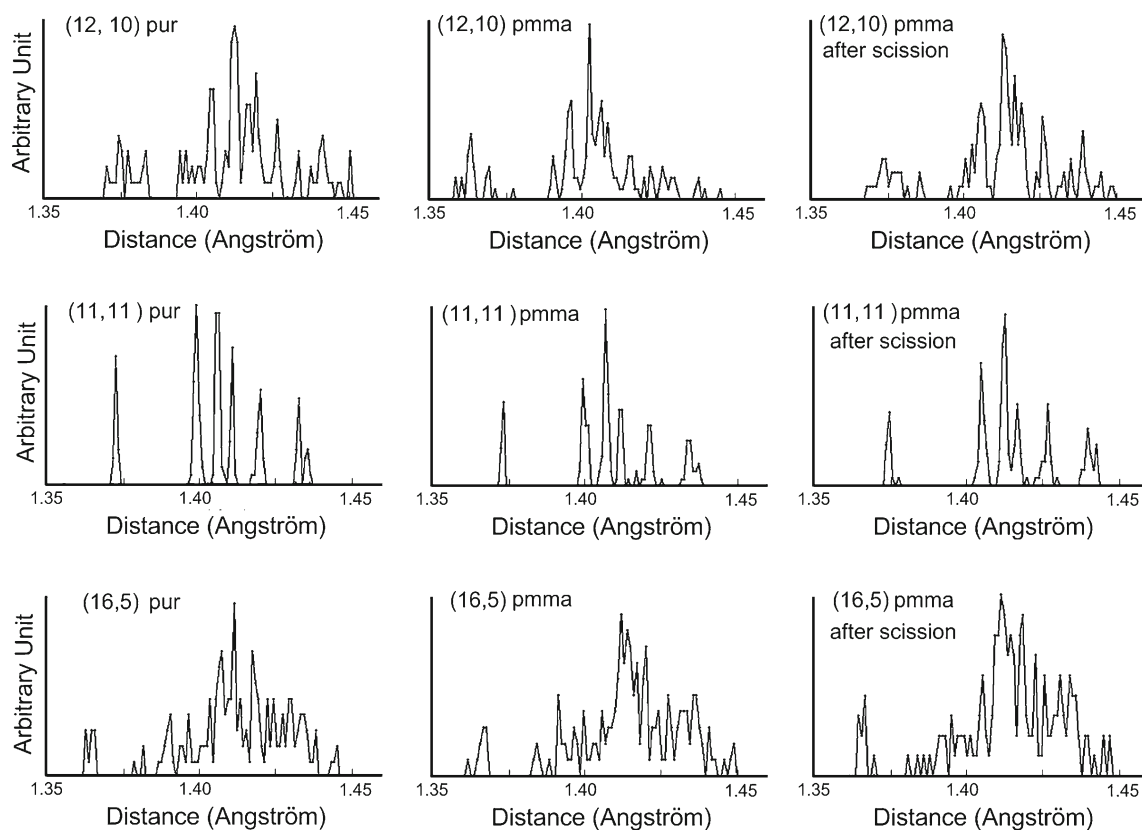


**Fig. 4** Distribution of carbon-carbon distances in pure and grafted carbon nanotubes

Thus, in saturated end groups without configuration defaults pure PMMA, the predominant mechanism of thermal degradation involves random main chain and side group scissions as proposed by Kashiwagi et al. [43–45] and Manring et al. [46]. The scission of bond 1 leads to a  $50 \text{ kJ mol}^{-1}$  more endothermic reaction than bond 2 for pure PMMA and (11,11). Consequently for these systems, the random bond scission first takes place in the backbone which could be later followed by a cleavage of the lateral bond as proposed by Kashiwagi et al. [43–45]. This difference is only around  $15 \text{ kJ mol}^{-1}$  for PMMA grafted on (12,10) and (16,5) nanotubes. So, if the thermal degradation is governed by the bond energies, the occurrences of a random chain scission and of a grafted side-group scission would be close for grafted PMMA on (12,10) and (16,5). Anyway, the grafting on carbon nanotubes introduces new weak bonds which are interesting to compare to weak bonds in polymer chain and known to affect the degradation temperature.

Unsaturated terminal groups and head to head configuration defaults are known to reduce the onset degradation temperature of PMMA even if their effect is still debatable [47]. Figure 5 displays the difference of BDE relative to the BDE (bond 2) of pure PMMA.

These results are in agreement with the thermal degradation of PMMA governed by bond energy for unsaturated

end group and head to head configuration defaults. Indeed, for low molecular mass PMMA in presence of head to head linkage, the onset degradation temperature is less than  $200 \text{ }^\circ\text{C}$  and with unsaturated end group it ranges from  $200 \text{ }^\circ\text{C}$  to  $300 \text{ }^\circ\text{C}$ , while it is higher than  $300 \text{ }^\circ\text{C}$  for random chain scission. From our results, the weakest bond was present in a head to head polymer model built from five repeated units and concerned the bond between two tertiary carbons on the main chain. The BDE of this bond was  $71 \text{ kJ mol}^{-1}$  less

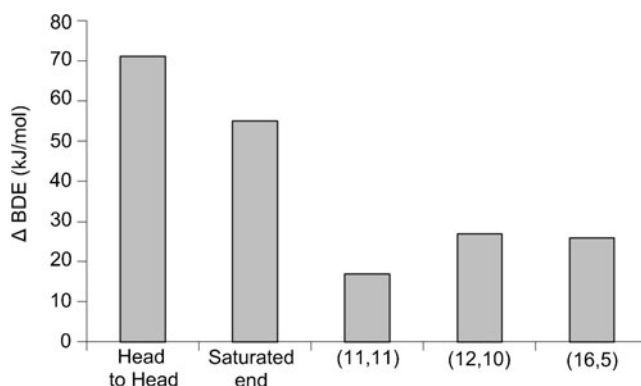


**Fig. 5**  $\Delta \text{BDE}(0 \text{ K}) \text{ (kJ mol}^{-1}\text{)}$  of bond 2 (bond 2' for unsaturated end) for different structural defects in comparison to the reference for pure PMMA ( $\Delta \text{BDE}(0 \text{ K})=0 \text{ kJ mol}^{-1}$ )

endothermic than the BDE (bond 2) of pure PMMA. In comparison, the BDE (bond 4) of the unsaturated end group was  $55 \text{ kJ mol}^{-1}$  less endothermic. It's worth noting that this difference is quite similar to the  $60 \text{ kJ mol}^{-1}$  difference in the activation energies for chain end and chain scission initiated degradation processes experimentally evaluated by Holland et al. [48]. The influence of PMMA grafted on carbon nanotube was less important than those two defaults since a difference of less than  $30 \text{ kJ mol}^{-1}$  was noted. Consequently, it can be inferred that these weak bonds (grafting defaults), if they exist in real PMMA/CNT systems, were not the main cause in the reduction of the ignition time observed for PMMA with 02 % and 1 % of CNT in comparison to pure PMMA [15]. The thermal conductivity of carbon nanotubes, higher than that of PMMA, can also be an influent factor on ignition time reduction. Moreover, it is important to notice that the thermal degradation is complex and can also be governed by structural and kinetic factors that were not covered in this study.

## Conclusions

In this study, a PMMA model of five repeat units was used to obtain qualitative results on the bond dissociation energies of a pure and a carbon nanotube grafted PMMA. Based on the results obtained on bond dissociation energies, we concluded that the error deviation on the calculated results, due to the configurations, was much lower than the experimental accuracy. In addition, we used a finite size model of carbon nanotubes for which the size can be regarded as sufficient. The validation of the model was based on the variation of the carbon carbon distances in pure and grafted carbon nanotubes and the electrostatic potential. The bond dissociation energies for grafted PMMA were less endothermic than that for pure PMMA. However, they are still more endothermic than those of head to head linkages or scissions at unsaturated ends possibly present in PMMA. This model was a first attempt to obtain an insight into the complex phenomena occurring in nanocomposites during the initial steps of thermal degradation. The challenge was to accurately evaluate the different energies involved in degradation processes, taking into account the numerous configurations and the steric effects due to the polymer chains. The improvements in supercomputers and simulation methods are useful but thoughts about the mechanisms of reactions and the creation of adequate models remain challenging.

**Acknowledgments** We thank ANR "Agence Nationale de la Recherche" for its sponsorship to the NANOFEU project (2008–2011) and partners (Institut National de l'Environnement Industriel et des Risques (INERIS), Laboratoire National de Métrologie et d'Essais (LNE), Ecole des Mines d'Alès (EMA), and PlasticsEurope). B. Minisini thanks particularly Grégoire Thiery and Bruno Stefani for their help.

## References

- Lu SY, Hamerton I (2002) *Prog Polym Sci* 27:1661–1712
- Laoutid F, Bonnaud L, Alexandre M, Lopez-Cuesta JM, Dubois P (2009) *Mater Sci Eng R* 63:100–125
- Weil ED (2011) *J Fire Sci* 29:259–296
- Shaw SD, Blum A, Weber R, Kannan K, Ritch D, Lucas D, Koshland CP, Dobraca D, Hanson S, Birnbaum LS (2010) *Rev Environ Health* 25:261–305
- Levchik SV, Weil ED (2006) *J Fire Sci* 24:345–364
- Kashiwagi T, Gilman JW (2000) Silicon-based flame retardants. In: Grand AF, Wilkie CA (eds) *Fire retardancy of polymeric materials*. Dekker, New York, pp 353–389
- Hollingbery LA, Hull TR (2010) *Polym Degrad Stab* 95:2213–2225
- Lewin M (2001) *Polym Adv Technol* 12:215–222
- Ma HY, Song PA, Fang ZP (2011) *Sci China Chem* 54:302–313
- Isitman NA, Kaynak C (2010) *Polym Degrad Stab* 95:1523–1532
- Lu H, Wilkie C (2010) *Polym Degrad Stab* 95:564–571
- Peeterbroeck S, Laoutid F, Swoboda B, Lopez-Cuesta JM, Moreau N, Nagy JB, Alexandre M, Dubois P (2007) *Macromol Rapid Commun* 28:260–264
- Cipriano BH, Kashiwagi T, Raghavan SR, Yang Y, Grulke EA, Yamamoto K, Shields JR, Douglas JF (2007) *Polymer* 48:6086–6096
- Costache MC, Wang D, Heidecker MJ, Manias E, Wilkie CA (2006) *Polym Adv Technol* 17:272–280
- Chivas-Joly C, Guillaume E, Ducourtieux S, Saragoza L, Lopez-Cuesta JM, Longuet C, Duplantier S, Bertrand J, Calogine D, Minisini B (2010) Influence of carbon nanotubes on fire behavior and on decomposition products of thermoplastic polymers. In: Grayson S (ed) *Interflam 2010: Proceedings of the 12th international conference, 5–7 July 2010*, Interscience communications, p 95–106
- Motzkus C, Chivas-Joly C, Guillaume E, Ducourtieux S, Saragoza L, Lesenechal D, Macé T, Lopez-Cuesta JM, Longuet C (2012) *J Nanoparticle Res* 14:1–17
- Quach Y, Cinausero N, Sonnier R, Longuet C, Lopez-Cuesta JM (2012) Barrier effect of flame retardant systems in poly(methyl methacrylate): study of the efficiency of the surface treatment by octylsilane of silica nanoparticles in combination with phosphorous fire retardant additives. *Fire Mater* doi:10.1002/fam.1119
- Kashiwagi T, Fagan J, Douglas JF, Yamamoto K, Heckert AN, Leigh SD, Obrzut J, Du F, Lin-Gibson S, Mu M, Winey KI, Haggenueller R (2007) *Polymer* 48:4855–4866
- Kashiwagi T, Mu M, Winey K, Cipriano B, Raghavan SR, Pack S, Rafailovich M, Yang Y, Grulke E, Shields J, Harris R, Douglas J (2008) *Polymer* 49:4358–4368
- Liu J, Rasheed A, Minus ML, Kumar S (2009) *J Appl Polym Sci* 112:142–156
- Zeng WR, Li SF, Chow WK (2002) *J Fire Sci* 20:401–433
- Kashiwagi T, Grulke E, Hilding J, Harris R, Awad W, Douglas J (2002) *Macromol Rapid Commun* 23:761–765
- Jia Z, Wang Z, Xu C, Liang J, Wei B, Wu D, Zhu S (1999) *Mater Sci Eng, A* 271:395–400
- Park SJ, Cho MS, Lim ST, Choi HJ, Jhon MS (2003) *Macromol Rapid Commun* 24:1070–1073
- Tasis D, Tagmatarchis N, Bianco A, Prato M (2006) *Chem Rev* 106:1105–1136
- Banerjee S, Hemraj-Benny T (2005) *Adv Mater* 17:17–29
- Laachachi A, Ferriol M, Cochez M, Ruch D, Lopez-Cuesta JM (2008) *Polym Degrad Stab* 93:1131–1137
- Van Krevelen DW (1990) *Properties of polymers*, 3rd edn. Elsevier, Amsterdam, Chapter 21
- Abate L, Blanco I, Orestano A, Pollicino A, Recca A (2003) *Polym Degrad Stab* 80:333–338
- Walters RN, Hackett SM, Lyon RR (2000) *Fire Mater* 24:245–252

31. Staggs JEJ (2004) *Fire Saf J* 39:711–720
32. [www.accelrys.com](http://www.accelrys.com)
33. Sun H (1998) *J Phys Chem B* 102:7338–7364
34. Delley B (1990) *J Chem Phys* 92:508–517
35. Delley B (2000) *J Chem Phys* 113:7756–7764
36. Raffi-Tabar H (2004) *Phys Rep* 390:235–452
37. Hohenberg P, Kohn W (1964) *Phys Rev B* 136:864–871
38. Kohn W, Sham LJ (1965) *Phys Rev A* 140:1133–1138
39. Vosko SH, Wilk L, Nusair M (1980) *Can J Phys* 58:1200–1211
40. Stoliarov SI, Westmoreland PR, Nyden MR, Forney GP (2003) *Polymer* 44:883–894
41. Conforti PF, Garrison BJ (2005) *Chem Phys Lett* 409:294–299
42. Stauffer E (2003) *Sci Justice* 43:29–40
43. Kashiwagi TT, Inaba A, Brown JE, Hatada K, Kitayama T, Masuda E (1986) *Macromolecules* 19:2160–2168
44. Inaba A, Kashiwagi T, Brown EJ (1988) *Polym Degrad Stab* 21:1–20
45. Kashiwagi T, Inaba A (1989) *Polym Degrad Stab* 26:161–184
46. Manring L (1991) *Macromolecules* 24:3304–3309
47. Ferriol M, Gentilhomme A, Cochez M, Oget N, Mieloszynski JL (2002) *Polym Degrad Stab* 79:271–281
48. Holland BJ, Hay JN (2001) *Polymer* 42:4825–4835